PREDICTION AND OPTIMIZATION OF MICROHARDNESS AND CORROSION BEHAVIOUR OF CuNi-Gr COMPOSITE COATINGS

Ajay PINGALE[1,*], Anil KATARKAR[2], Masnaji NUKULWAR[1], Sachin BELGAMWAR[3], Jitendra S. RATHORE[3]

Graphene nanoplatelets (Gr) as fillers for alloy composite coatings has increased due to their remarkable high aspect ratio and distinctive plate-like structure. Piping, condensers and heat exchangers in seawater systems, desalination plants, marine hardware and boat hulls are expected to exhibit high wear and corrosion resistance. For this purpose, CuNi-Gr composite coatings have been fabricated using electrodeposition technique and investigated their microhardness and anti-corrosion properties. During the electrodeposition of coatings, the various process variables such as pH, current density, Gr concentration and amount of nickel sulfate have been taken into account. To achieve the full potential of CuNi-Gr composite coating in engineering applications, this study optimizes the performance of the CuNi-Gr composite coating using an orthogonal array design of a Taguchi technique. By Taguchi and regression analysis, it was found that the Gr concentration in the electrolyte is the most influencing parameter of the process for microhardness and polarization resistance of the CuNi-Gr composite coatings. It has been observed that the microhardness and polarization resistance of the composite coatings increase with the increase in the Gr content up to 400 mg/L.

Keywords: Alloy; Composite; Corrosion; Graphene; Microhardness

1. Introduction

Nanotechnology and nanoscience have become subjects of great interest in research due to their extensive applications and numerous advantages in various engineering sectors [1–3]. Nanoparticles are characterized as particles with at least one dimension measuring less than 100 nm [4]. When the size of a material falls within the range of 1-100 nm, its properties can exhibit significant changes, leading to exceptional characteristics. Nanomaterials possess distinct properties compared to their macro counterparts. Many natural nanoparticles are present in the volcano dust, soil, seawater spills, humid matter, colloidal clay, soil, and atmosphere on the earth [5]. Nanomaterials produced through nanotechnology exhibit enhanced

[1] Department of Mechanical Engineering, PCET's Pimpri Chinchwad College of Engineering, Pune, India, e-mail: ajay.pingale@pccoepune.org
[2] Department of Mechanical Engineering, NIT Agartala, Tripura , India
[3] Department of Mechanical Engineering, BITS Pilani, Pilani, India

flexibility, strength, and surface-to-volume ratio. The atoms located on the surface of nanoparticles tend to be more reactive compared to other atoms. Nanoparticles in powder form can be utilized as catalysts or solid fuels in rocket applications. [6]. Nanoparticles are widely used in electronics, optics, medicine, chemistry, agricultural, food, and automobile industries [7]. Graphene, carbon nanotube (CNT), and c60 fullerene are 2-, 1- and 0-dimensional nanomaterials, respectively, and their properties are not similar to macroscopic carbon materials. The unexpected properties of nanocarbon have a novel scientific field that can drastically change our lifestyle. Among the various types of nanoparticles, graphene has been paid special attention.

Graphene is a crystalline lattice structure consisting of carbon atoms arranged in a one-atom-thick planar sheet, exhibiting greater strength than diamond [8]. The mechanical exfoliation method was first employed in 2004 to isolate graphene from graphite [9–12]. Over time, several methods have been developed to produce graphene, including exfoliation and cleavage, thermal chemical vapor deposition, plasma-enhanced chemical vapor deposition, thermal decompositions, electrochemical methods, and pulsed-laser scribing [13]. The exceptional properties of graphene, such as its large theoretical specific surface area, excellent electrical conductivity, and high mechanical strength, have attracted significant research interest in recent years [14]. It's remarkable electronic, mechanical, optical, electrochemical, and thermal properties, compared with other carbon materials, make it a promising material in electrical, chemical and automobile industrial applications [12, 15–17]. Graphene nanoplatelets (Gr) consist of a few layers of graphene and possess several superior properties, including super charge-carrier mobility (200,000 cm^2/Vs), high Young's modulus (1 TPa), extreme thermal conductivity (5,000 W/mK), and a higher fracture toughness of 125 GPa [18]. Gr have found wide applications in the electronic industries due to its superior carrier mobility (up to 350,000 cm^2 /Vs) and high optical transparency (97.7%) [19].

The advantage of graphene over CNT using in composites includes high-pressure processing result in damage to CNT structure; the possibility of graphene to disperse uniformly in the metal matrix without agglomeration; short CNT serve as a good reinforcing element however, not suitable for wear applications, CNT forms only point to point contact however, graphene has strong interfacial bonding, fracture strengthening is more in graphene composites because of its planar geometry and high aspect ratio [20–25]. These extraordinary properties make graphene an ideal reinforcing material for the composites, possibly enhancing the resulting composite's mechanical, tribological and corrosion properties. To have the advantage of their extraordinary properties at the bulk level, scientists are exploring the possibility of preparing composites, termed as graphene-reinforced composites.

Graphene is very light in weight and cannot be dissolved in water, and it can be dispersed uniformly in a plating solution using a surfactant [26, 27]. Recently

graphene gained extensive interest in the electrochemistry field and has many applications in various sectors like biosensors [28], supercapacitors [29], transparent electrodes [30], sensors [31], nanoscale electronic devices [32], and field emission devices [33] and filler materials [34]. Owing to the outstanding properties of graphene, it is believed that it could significantly improve the performance of composites. Also, graphene is ideal to be an efficient reinforcing element to achieve high-quality metal matrix composite coatings.

Alloy deposition is an old technique and same scientific principles as individual metals electrodeposition [35–38]. The interest in the utilization of alloy coating is increased due to the wide range of possible alloy combinations and the related possible applications. Alloy coatings have superior properties in certain composition ranges than those of individual metal coatings [39–41]. They can be harder, have better resistance against corrosion, stronger and tougher, more wear resistance and superior in magnetic properties. CuNi alloy coatings are widely used to reduce corrosion and wear rate. Hence, it finds many applications in piping, condensers and heat exchangers in seawater systems, desalination plants, marine hardware and boat hulls [42–44]. The incorporation of Gr into CuNi alloy coating has augmented the mechanical and corrosion resistance properties of resulting coatings as compared to pure CuNi alloy coating [45, 46].

In the present work, to address the demanding wear and corrosion requirements of seawater systems, desalination plants, marine hardware, and boat hulls, CuNi-Gr composite coatings were fabricated using an electrodeposition technique. The effects of various process parameters, including pH, current density, graphene concentration, and nickel sulfate amount, on the coatings' microhardness and anti-corrosion properties were systematically investigated and optimized. Our findings offer a practical roadmap for optimizing properties of CuNi-Gr coatings for enhanced service life and reduced maintenance costs in marine environments, contributing to enhanced sustainability and operational efficiency.

2. Fabrication of Coatings

The reagents used in the study were of analytical grade with a purity of 99% and were supplied by Merck Specialties Pvt. Ltd. All electrolyte solutions were prepared using deionized (DI) water. A 250 cm^3 volume of the citrate bath consisted of copper sulfate pentahydrate ($CuSO_4.5H_2O$) as the source of copper, nickel sulfate hexahydrate ($NiSO_4.6H_2O$) as the source of nickel, and trisodium citrate dihydrate ($Na_3C_6H_5O_7.2H_2O$) as a complex agent. Sulfuric acid (H_2SO_4) was used to adjust the pH of the electrolyte solution. The graphene used in the coatings was reduced graphene oxide with a surface area of 500 m^2/g, obtained from Alfa Aesar. For detailed information on the fabrication process and characterization of CuNi-Gr composite coatings, please refer to our previous work [45, 46].

3. Characterization of Coatings

Surface microhardness measurements of coatings were performed on a Vickers hardness tester (Mitutoyo HM-200) using a 20 g-f load for 10 seconds. Five measurements were conducted on each sample. The corrosion performance of the coatings was evaluated using a CHI604E potentiostat workstation at room temperature in a 3.5 wt.% NaCl solution. The CuNi-Gr coating, Ag/AgCl electrode, and Pt wire were used as the working electrode, reference electrode, and counter electrode, respectively.

4. Experimental design

In this study, several process variables were chosen, including pH, current density, Gr concentration, and the amount of nickel sulfate. The fixed electrolysis parameters for the experimental investigation can be found in Table 1. The selected ranges for each process variable are listed in Table 2. The experimental design was based on the Taguchi method, and the results were analyzed to determine the microhardness values of the composite coating.

Table 1.

Fixed electrolysis parameter for experimental study

Fixed Parameters	Quantity
Amount of $CuSO_4.5H_2O$	21 g/L
Electrodeposition Time	60 min
Magnetic stirring	350 rpm
Ultrasonication time	60 min

The significance of each parameter was ranked based on the results of the aforementioned studies. Analysis of variances (ANOVA) was conducted to assess the significance of the process parameters, and the percentage of contributions was determined. For this study, the maximum hardness and high polarization resistance (Rp) were chosen as the performance index. A larger-the-better S/N ratio was selected for evaluating both microhardness and polarization resistance.

$$\frac{S}{N} = -10\, log\, \frac{1}{N_i} \sum \frac{1}{y_i^2} \tag{1}$$

where, $y_i$denotes the N_i observations of response variables. In electro-co-deposition method, major parameters, which influence the quality of prepared CuNi-Gr composite coating are 1) pH, 2) current density, 3) Gr concentration in the electrolyte and 4) amount of nickel sulfate. With the four parameters as variables

and considering four levels of each variable, a fractional factorial design of 16 experiments is done with L_{16} orthogonal array.

Table 2 presents the respective process variable with their corresponding levels with which the composite coatings have been experimented and optimization of microhardness and polarization resistance using Taguchi was performed using MINITAB software. The experiments have been conducted using Taguchi experimental design (L_{16} orthogonal array) and are listed in Table 3.

Table 2.

Input variables and their levels.

Parameter	Description	Level 1	Level 2	Level 3	Level 4
A	pH	3	3.5	4	4.5
B	Current density (A/dm^2)	2	4	6	8
C	Gr concentration (mg/L)	100	200	300	400
D	$NiSO_4.6H_2O$ (g/L)	42	63	84	105

5. Statistical analysis of experimental results

Statistical modeling has been conducted to assess the microhardness and polarization resistance of CuNi-Gr composite coatings synthesized via the electrodeposition method. First-order models were developed to estimate the microhardness and polarization resistance of the coatings. These models were generated through regression analysis of the experimental data, which can be found in Table 3.

Statistical analysis was performed on the microhardness of the coatings across three sets of sixteen experiments. The results of this analysis can be found in Table 4. Variance analysis, utilizing the Taguchi method with significant values of process parameters, was employed to analyze the microhardness. The findings from this analysis are provided in Table 4.

The regression analysis was conducted to derive the model, represented by the following equation (2):

$$\text{Microhardness} = 275.6 - 1.35\,A + 0.41\,B + 0.3392\,C + 0.651\,D \qquad (2)$$

where, microhardness in HV, A is the pH, B is the current density (A/dm^2), C is the amount of Gr concentration (mg/L) and D is the amount of nickel sulfate (g/L). Fig. 1 presents two graphical representations: (a) a main effect plot illustrating the influence of process parameters on the alteration of microhardness (HV), and (b) a breakdown of the percentage contribution of these process parameters to the change in microhardness (HV). The main effect plot reveals that within the studied parameters (pH 3-4.5, current density 2-8 A/dm^2, and nickel sulfate concentration 42-105 g/L), factors like pH, current density, and nickel

sulfate concentration did not significantly influence the microhardness of the CuNi-Gr composite coatings. Notably, the concentration of graphene (Gr) in the electrolyte bath (100-400 mg/L) emerged as the most impactful parameter controlling microhardness. This effect can be attributed to Gr providing preferential sites for crystal growth of the CuNi alloy during deposition, leading to a decrease in average crystallite size [10]. The increased microhardness of the CuNi-Gr composite coatings observed with increasing Gr concentration up to 400 mg/L is likely due to this combined effect of reduced crystallite size and the extraordinary properties of Gr [10].

Table 3.

The basic Taguchi L16 orthogonal array

Exp. No.	Parameters				Notation	Microhardness (HV)	R_p ($k\Omega.cm^2$)
	A	B	C	D			
1	1	1	1	1	$A_1B_1C_1D_1$	374	94.23
2	1	2	2	2	$A_1B_2C_2D_2$	423	151.65
3	1	3	3	3	$A_1B_3C_3D_3$	454	188.87
4	1	4	4	4	$A_1B_4C_4D_4$	482	223.35
5	2	1	2	3	$A_2B_1C_2D_3$	432	156.87
6	2	2	1	4	$A_2B_2C_1D_4$	388	123.74
7	2	3	4	1	$A_2B_3C_4D_1$	458	204.41
8	2	4	3	2	$A_2B_4C_3D_2$	435	177.85
9	3	1	3	4	$A_3B_1C_3D_4$	458	190.41
10	3	2	4	3	$A_3B_2C_4D_3$	475	217.32
11	3	3	1	2	$A_3B_3C_1D_2$	368	112.65
12	3	4	2	1	$A_3B_4C_2D_1$	398	145.45
13	4	1	4	2	$A_4B_1C_4D_2$	466	205.14
14	4	2	3	1	$A_4B_2C_3D_1$	427	169.43
15	4	3	2	4	$A_4B_3C_2D_4$	430	172.34
16	4	4	1	3	$A_4B_4C_1D_3$	372	115.73

Table 4.

Analysis of variance for microhardness

Source	DF	Adj SS	Adj MS	F-Value	P-Value	R^2
Regression	4	26780.9	6695.2	37.57	0.000	93.18%
A	1	9.1	9.1	0.05	0.825	
B	1	13.6	13.6	0.08	0.787	
C	1	23018.1	23018.1	129.15	0.000	
D	1	3740.1	3740.1	20.99	0.001	
Error	11	1960.5	178.2			
Total	15	28741.4				

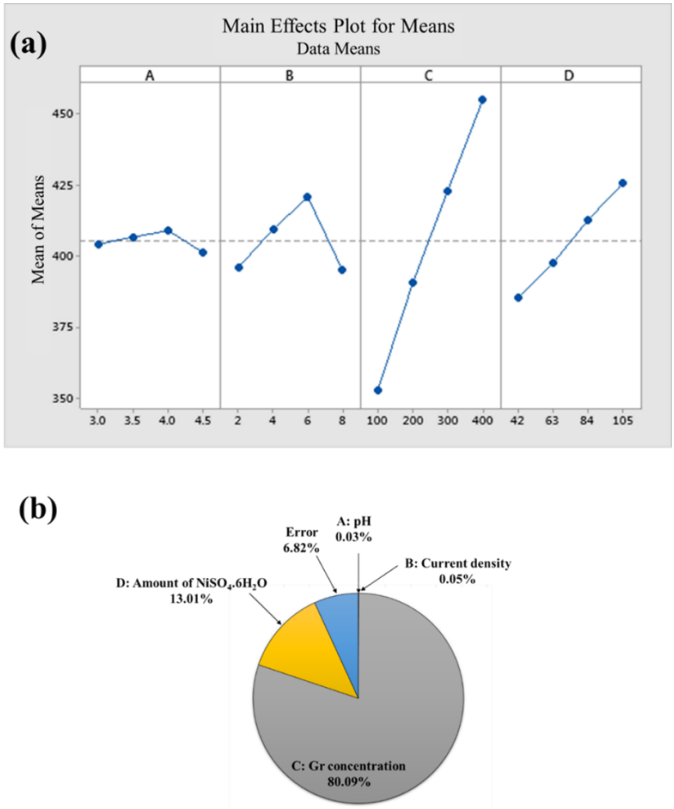

Fig. 1. (a) Main effect plot illustrating the influence of process parameters on the alteration of microhardness (HV), (b) Breakdown of the percentage contribution of these process parameters to the change in microhardness (HV)

Table 5 presents the results of the variance analysis conducted to investigate the polarization resistance. The analysis was carried out using the Taguchi method, considering significant values of process parameters. The obtained data from this analysis are listed in Table 5.

Table 5.

Analysis of variance for polarization resistance

Source	DF	Adj SS	Adj MS	F-Value	P-Value	R^2
Regression	4	22849.4	5712.4	152.93	0.00000	98.23%
A	1	3.4	3.4	0.09	0.76732	
B	1	50.1	50.1	1.34	0.27126	
C	1	21512.2	21512.2	575.92	0.00000	
D	1	1283.7	1283.7	34.37	0.00011	
Error	11	410.9	37.4			
Total	15	23260.3				

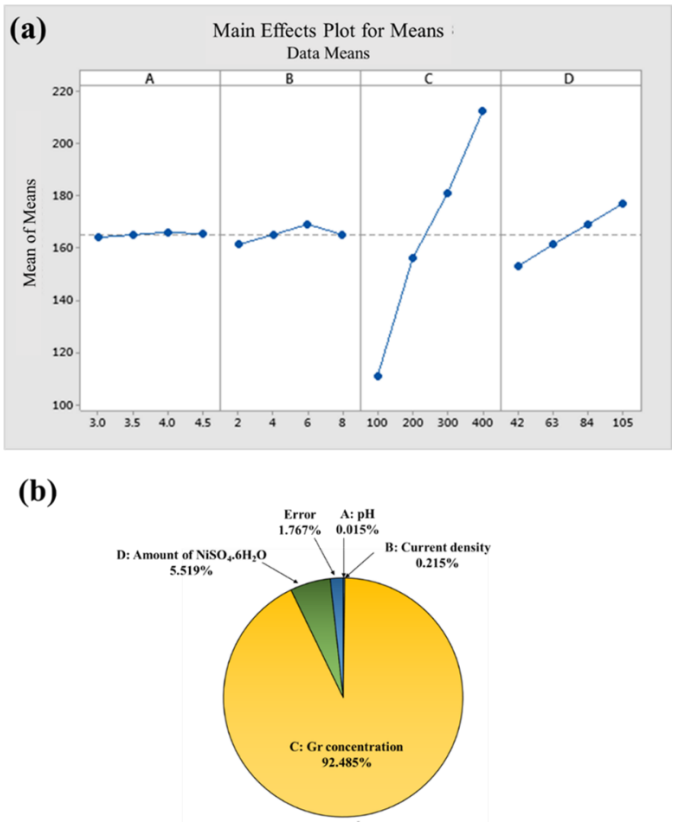

Fig. 2. (a) Main effect plot demonstrating the impact of process parameters on the alteration of polarization resistance (kΩ.cm^2), (b) Main effect plot demonstrating the impact of process parameters on the alteration of polarization resistance (kΩ.cm^2)

The regression analysis was conducted to derive the model, represented by the following equation (3):

$$R_p = 48.5 + 0.83\ A + 0.791\ B + 0.3280\ C + 0.3815\ D \quad (3)$$

where, R_p represents polarization resistance in kΩ.cm^2, A is the pH, B is the current density (A/dm^2), C is the amount of Gr concentration (mg/L) and D is the amount of nickel sulfate (g/L). Fig. 2 illustrates two graphical representations: (a) a main effect plot demonstrating the impact of process parameters on the alteration of polarization resistance (kΩ.cm^2), and (b) a breakdown of the percentage contribution of these process parameters to the change in polarization resistance (kΩ.cm^2).

The main effect plot reveals that pH, current density, and the amount of nickel sulfate exhibit negligible influence on the polarization resistance within the considered range of process parameters. However, the main effect plots indicate that the concentration of Gr in the electrolyte bath emerges as the most significant

process parameter affecting the polarization resistance of CuNi-Gr composite coatings.

To validate the developed regression model, a limited number of experiments were conducted using random values for the process parameters. The results of these experiments are presented in Table 6.

Table 6.

Experimental validation results

Sr. No	Process Parameters				Microhardness (HV)		R_p (kΩ.cm^2)	
	A	B	C	D	Regression predicted	Experimental	Regression predicted	Experimental
1	3	2	100	63	347 ± 23	356	109.40 ± 1.9	113.12
2	4	8	300	42	402 ± 24	412	172.52 ± 3.0	169.25
3	4.5	4	200	84	393 ± 23	381	153.04 ± 2.7	156.46

The optimized values of process parameters for the maximum value of the microhardness and polarization resistance are listed in Table 7.

Table 7.

The optimized values of process parameters for the maximum value of the microhardness and polarization resistance of CuNi-Gr composite coating

Parameter No.	Description	Value
A	pH	4
B	Current density (A/dm^2)	6
C	Gr concentration (mg/L)	400
D	$NiSO_4.6H_2O$ (g/L)	105

CuNi-Gr composite coatings are fabricated by electro-co-deposition method and tested for microhardness and polarization resistance. The microhardness and polarization resistance of coatings are investigated by using a microhardness tester and potentiostat, respectively. All prepared coatings are tested under identical conditions in a controlled environment. The results revealed that the microhardness and polarization resistance of the CuNi-Gr composite coating increases with an increase in the Gr concentration in the electrolyte bath. By Taguchi and regression analysis, it is found that the Gr concentration in the electrolyte is the most influencing parameter of the process for microhardness and polarization resistance of the CuNi-Gr composite coatings. The addition of Gr decreases the crystallite size of the coating and hence requires more power for penetration, which results in a rise in microhardness [45]. More concentration of the nickel sulfate in the electrolyte increases the amount of Ni in the CuNi-Gr composite coatings and improves the microhardness value. Also, graphene nanoplatelets act as an inert

physical barrier to the initiation and growth of corrosion defects, improving corrosion resistance [47].

6. Conclusion

A statistical approach combining Taguchi and variance analysis was employed to investigate the influence of electrolysis parameters on the mechanical and corrosion properties of CuNi-Gr composite coatings. The findings revealed that parameters such as solution pH and current density had minimal impact on the microhardness and corrosion resistance of the CuNi-Gr coatings. The incorporation of graphene (Gr) into the coatings reduced the crystallite size, necessitating increased power for penetration, consequently leading to higher microhardness. Moreover, higher concentrations of nickel sulfate in the electrolyte resulted in increased nickel content within the CuNi-Gr coatings, thereby enhancing the microhardness. Additionally, graphene nanoplatelets acted as a protective barrier, effectively preventing the initiation and propagation of corrosion defects and thereby improving corrosion resistance. The most significant improvements in microhardness (482 HV) and corrosion resistance (R_p = 223 kΩ.cm^2) of CuNi-Gr composite coating were observed at a pH value of 4, a current density of 8 A/dm^2, a Gr concentration of 400 mg/L, and an amount of $NiSO_4 \cdot 6H_2O$ in the plating bath of 105 g/L.

REFERENCES

[1] *R.S. Bhat, K.B. Manjunatha, R. P. Shankara, et al.* "Electrochemical studies on the corrosion resistance of Zn–Ni–Co coating from acid chloride bath", in Appl. Phys. A, Oct. 2020, **vol. 126**, pp. 772.

[2] *R.S. Bhat, S.M Shetty, N.A. Kumar*. "Electroplating of Zn-Ni Alloy Coating on Mild Steel and Its Electrochemical Studies", in J. Mater. Eng. Perform., Nov. 2021, **vol. 30**, pp. 8188–8195.

[3] *R.S. Bhat, P. Nagaraj, S. Priyadarshini*. "Zn–Ni compositionally modulated multilayered alloy coatings for improved corrosion resistance", in Surf. Eng., Jun. 2021, **vol. 37**, pp. 755–763.

[4] *C.M. Hussain* "Nanomaterials in Chromatography: Current Trends in Chromatographic Research Technology and Techniques", in Elsevier Science, 2018.

[5] *H.A. Khan, I.A. Arif*. "Toxic Effects of Nanomaterials", in Bentham Science, 2012,

[6] *D. Shi* "Nanomaterials and Devices", in Elsevier Science, 2014

[7] *S. Kanchi, S. Ahmed*. "Green Metal Nanoparticles: Synthesis, Characterization and their Applications", in Wiley, 2018.

[8] *M. Skoda, I. Dudek, A. Jarosz, et al.* "Graphene: One Material, Many Possibilities—Application Difficulties in Biological Systems", in J. Nanomater., 2014, **vol. 2014**, pp. 1–11.

[9] *J. Park, H. Elmlund, P. Ercius, et al.* "3D structure of individual nanocrystals in solution by electron microscopy", in Science, Jul. 2015, **vol. 349**, pp. 290–295.

[10] *A.R. Shelke, J. Balwada, S. Sharma, et al.* "Development and characterization of Cu-Gr

composite coatings by electro-co-deposition technique", in Mater. Today Proc., Apr. 2020, **vol. 28**, pp. 2090–2095.

[11] *A.D. Pingale, S.U. Belgamwar, J.S. Rathore*. "A novel approach for facile synthesis of Cu-Ni/GNPs composites with excellent mechanical and tribological properties", in Mater. Sci. Eng. B, Oct. 2020, **vol. 260**, pp. 114643.

[12] *A. Owhal, A. Pingale, S. Belgamwar*. "Developing sustainable Zn-MWCNTs composite coatings using electrochemical co-deposition method: Tribological and surface wetting behavior", in Adv. Mater. Process. Technol., Nov. 2022, **vol. 8**, pp. 2142–2155.

[13] *Choi W., I. Lahiri, R. Seelaboyina, et al.* "Synthesis of Graphene and Its Applications: A Review", in Crit. Rev. Solid State Mater. Sci., Feb. 2010, **vol. 35**, pp. 52–71.

[14] *Allen M.J., V.C. Tung, R.B. Kaner*. "Honeycomb Carbon: A Review of Graphene", in Chem. Rev., Jan. 2010, **vol. 110**, pp. 132–145.

[15] *M.S. Fuhrer, C.N. Lau, A.H. MacDonald*. "Graphene: Materially Better Carbon", in MRS Bull., Apr. 2010, **vol. 35**, pp. 289–295.

[16] *B. Majumder, A. Pingale, A. Katarkar, et al.* "Developing Al@GNPs composite coating for pool boiling applications by combining mechanical milling, screen printing and sintering methods", in Adv. Mater. Process. Technol., Nov. 2022, **vol. 8**, pp. 2110–2121.

[17] *A.S. Katarkar, A.D. Pingale, S.U. Belgamwar, et al.* "Fabrication of Cu@G composite coatings and their pool boiling performance with R-134a and R-1234yf", in Adv. Mater. Process. Technol., Nov. 2022, **vol. 8**, pp. 2044–2056.

[18] *C. Lee, X. Wei, J.W. Kysar, et al.* "Measurement of the Elastic Properties and Intrinsic Strength of Monolayer Graphene", in Science, Jul. 2008, **vol. 321**, pp. 385–388.

[19] *R.R. Nair, P. Blake, A.N. Grigorenko, et al.* "Fine Structure Constant Defines Visual Transparency of Graphene", in Science, Jun. 2008, **vol. 320**, pp. 1308–1308.

[20] *B. Majumder, A.D. Pingale, A.S. Katarkar, et al.* "Enhancement of Pool Boiling Heat Transfer Performance of R-134a on Microporous Al@GNPs Composite Coatings", in Int. J. Thermophys., Apr. 2022, **vol. 43**, pp. 49.

[21] *A.D. Pingale, A. Owhal, S.U. Belgamwar, et al.* "Co-deposited CuNi@MWCNTs nanocomposites for structural applications: tribo-mechanical and anti-corrosion performances", in Trans. IMF, Mar. 2023, **vol. 101**, pp. 93–100.

[22] *B. Majumder, A.D. Pingale, A.S. Katarkar, et al.* "Pool Boiling Heat Transfer Performance of R-134a on Microporous Al Surfaces Electrodeposited from AlCl3/Urea Ionic Liquid", in J. Eng. Thermophys., Dec. 2022, **vol. 31**, pp. 720–736.

[23] *S. Satpathy, M. Chandra Trivedi, V. Goyal, et al.* "Fractographic properties of electrode material of supercapacitor (carbon aerogel) with its application", in Adv. Mater. Process. Technol., 2021, **vol. 8**, pp. 685–695.

[24] *A.S. Katarkar, A.D. Pingale, S.U. Belgamwar, et al.* "An experimental study on pool boiling of R-600a on Cu@Gr composite-coated patterned surfaces", in J. Brazilian Soc. Mech. Sci. Eng., Jan. 2023, **vol. 45**, pp. 40.

[25] *X. M. Anthony, H.G. Prashantha Kumar*. "Processing and Characterization Techniques of Graphene Reinforced Metal Matrix Composites (GRMMC); A Review", in Mater. Today Proc., 2017, **vol. 4**, pp. 3334–3341.

[26] *C. Song, D. Wu, F. Zhang, et al.* "Gemini surfactant assisted synthesis of two-dimensional metal nanoparticles/graphene composites", in Chem. Commun., 2012, vol. **48**, pp. 2119.

[27] *M. Lotya, P.J. King, U. Khan, et al.* "High-Concentration, Surfactant- Stabilized Graphene Dispersions", in ACS Nano, 2010, **vol. 4**, pp. 3155–3162.

[28] *Y. Zhou, J. Yang, X. Cheng, et al.* "Electrostatic self-assembly of graphene-silver multilayer films and their transmittance and electronic conductivity", in Carbon N. Y., 2012, **vol. 50**, pp. 4343–4350.

[29] *Y. Dai, S. Cai, W. Yang, et al.* "Fabrication of self-binding noble metal/flexible graphene

composite paper", in Carbon N. Y., 2012, **vol. 50**, pp. 4648–4654.
[30] *B.G. Choi, J. Hong, W.H. Hong, et al.* "Facilitated Ion Transport in All-Solid- State Flexible Supercapacitors", in ACS Nano, 2011, vol. **5**, pp. 7205–7213.
[31] *N. Hu, Y. Wang, J. Chai, et al.* "Gas sensor based on p-phenylenediamine reduced graphene oxide", in Sensors Actuators, B Chem., 2012, **vol. 163**, pp. 107–114.
[32] *A.K. Geim, K.S. Novoselov*. "The rise of graphene", in Nat. Mater., Mar. 2007, **vol. 6**, pp. 183–191.
[33] *M.A. Raza, A. Westwood, A. Brown, et al.* "Characterisation of graphite nanoplatelets and the physical properties of graphite nanoplatelet/silicone composites for thermal interface applications", in Carbon N. Y., 2011, **vol. 49**, pp. 4269–4279.
[34] *J. Yan, T. Wei, B. Shao, et al.* "Preparation of a graphene nanosheet/polyaniline composite with high specific capacitance", in Carbon N. Y., 2010, **vol. 48**, pp. 487–493.
[35] *Schlesinger M., M. Paunovic*. "Modern Electroplating", in Wiley, 2011,
[36] *R.S. Bhat, S. Bekal, A.C. Hegde*. "Fabrication of Zn-Ni Alloy Coatings from Acid Chloride Bath and its Corrosion Performance", in Anal. Bioanal. Electrochem., 2018, **vol. 10**, pp. 1562–1573.
[37] *R.S. Bhat, V.B. Shet*. "Development and characterization of Zn–Ni, Zn–Co and Zn–Ni–Co coatings", in Surf. Eng., Apr. 2020, **vol. 36**, pp. 429–437.
[38] *S. Bhat, K. Venkatakrishna, J Nayak, et al.* "Compositionally Modulated Multilayered Zn-Co Deposits for Better Corrosion Resistance", in J. Mater. Eng. Perform., Oct. 2020, **vol. 29**, pp. 6363–6371.
[39] *A. Owhal, A.D. Pingale, S.U. Belgamwar, et al.* "Preparation of novel Zn/Gr MMC using a modified electro-co-deposition method: Microstructural and tribo-mechanical properties", in Mater. Today Proc., Nov. 2020, **vol. 44**, pp. 222–228.
[40] *A. Owhal, A.D. Pingale, S.U. Belgamwar, et al.* "A brief manifestation of anti-bacterial nanofiller reinforced coatings against the microbial growth based novel engineering problems", in Mater. Today Proc., 2021, **vol. 47**, pp. 3320–3330.
[41] *A. Owhal, A.D. Pingale, S. Khan, et al.* "Electro-codeposited γ-Zn-Ni/Gr composite coatings: Effect of graphene concentrations in the electrolyte bath on tribo-mechanical, anti-corrosion and anti-bacterial properties", in Trans. IMF, Oct. 2021, **vol. 99**, pp. 1–8.
[42] *J. Ahmed, K. V. Ramanujachary, S.E. Lofland, et al.* "Bimetallic Cu-Ni nanoparticles of varying composition (CuNi3, CuNi, Cu3Ni)", in Colloids Surfaces A Physicochem. Eng. Asp., 2008, **vol. 331**, pp. 206–212.
[43] *C.R. Thurber, Y.H. Ahmad, S.F. Sanders, et al.* "Electrodeposition of 70-30 Cu-Ni nanocomposite coatings for enhanced mechanical and corrosion properties", in Curr. Appl. Phys., 2016, **vol. 16**, pp. 387–396.
[44] *P.Q. Dai, C. Zhang, J.C. Wen, et al.* "Tensile Properties of Electrodeposited Nanocrystalline Ni-Cu Alloys", in J. Mater. Eng. Perform., Feb. 2016, **vol. 25**, pp. 594–600.
[45] *A.D. Pingale, S.U. Belgamwar, J.S. Rathore*. "Effect of Graphene Nanoplatelets Addition on the Mechanical, Tribological and Corrosion Properties of Cu–Ni/Gr Nanocomposite Coatings by Electro-co-deposition Method", in Trans. Indian Inst. Met., Jan. 2020, **vol. 73**, pp. 99–107.
[46] *A.D. Pingale, S.U. Belgamwar, J.S. Rathore*. "Synthesis and characterization of Cu–Ni/Gr nanocomposite coatings by electro-co-deposition method: effect of current density", in Bull. Mater. Sci., Dec. 2020, **vol. 43**, pp. 66.
[47] *M.E.Turan, Y. Sun, Y. Akgul, et al.* "The effect of GNPs on wear and corrosion behaviors of pure magnesium", in J. Alloys Compd., 2017, **vol. 724**, pp. 14–23.